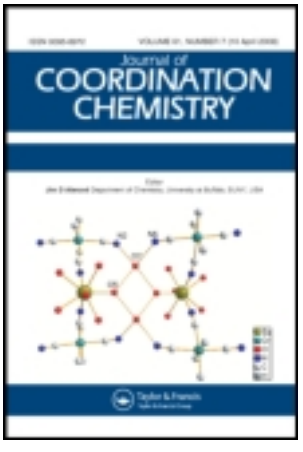

Journal of Coordination Chemistry
Publication details, including instructions for authors and subscription information:
http://www.tandfonline.com/loi/gcoo20

Hydrothermal synthesis and characterization of a new Anderson-type polyoxometalate

Rui Ran [a b], Haijun Pang [a], Zhigang Yu [a], Huiyuan Ma [a b] & Ye Xun [a]

[a] Key Laboratory of Green Chemical Engineering and Technology of College of Heilongjiang Province, College of Chemical and Environmental Engineering, Harbin University of Science and Technology, Harbin 150040, China

[b] Chemistry Department of Harbin Normal University, Harbin 150025, P.R. China

Published online: 12 Jul 2011.

To cite this article: Rui Ran, Haijun Pang, Zhigang Yu, Huiyuan Ma & Ye Xun (2011) Hydrothermal synthesis and characterization of a new Anderson-type polyoxometalate, Journal of Coordination Chemistry, 64:13, 2388-2398, DOI: 10.1080/00958972.2011.598230

To link to this article: http://dx.doi.org/10.1080/00958972.2011.598230

Journal of Coordination Chemistry
Vol. 64, No. 13, 10 July 2011, 2388–2398

Hydrothermal synthesis and characterization of a new Anderson-type polyoxometalate

RUI RAN†‡, HAIJUN PANG†, ZHIGANG YU†, HUIYUAN MA*†‡ and YE XUN†

†Key Laboratory of Green Chemical Engineering and Technology of College of Heilongjiang Province, College of Chemical and Environmental Engineering, Harbin University of Science and Technology, Harbin 150040, China
‡Chemistry Department of Harbin Normal University, Harbin 150025, P.R. China

(*Received 9 November 2010; in final form 25 May 2011*)

A new compound based on Anderson-type polyoxometalate, $[Cu(phen)H_2O]_2[CrH_5Mo_6O_{24}]\cdot 5H_2O$ (**1**) (phen = 1,10-phenanthroline), has been hydrothermally synthesized and characterized by single-crystal X-ray diffraction, elemental analysis, IR spectrum, and thermal gravimetric analysis. Luminescent, electrochemical, and electroactivity properties of **1** have been studied.

Keywords: Polyoxometalate; Hydrothermal synthesis; Anderson structure; Electroactivity

1. Introduction

The design and synthesis of polyoxometalates (POMs) attract interest for their structural and topological novelty and their potential applications in catalysis, magnetism, medicinal chemistry, functional materials, etc. [1–4]. POMs are usually employed as inorganic building blocks connecting metal complexes to construct organic–inorganic hybrid materials. The classical Keggin [5a, 5b], Wells–Dawson [5c], and Lindquist [6] polyoxoanions have been extensively studied. In contrast, the use of Anderson polyoxoanions as inorganic building blocks is largely unexplored. Anderson polyoxoanions possess planar structures and each molybdenum has two terminal oxygens with high reactivity [7, 8]. Therefore, the Anderson polyoxoanions are good candidates as multidentate ligands to link transition or rare-earth metal complexes and facilitate the construction of organic–inorganic hybrid compounds. Most reported hybrid compounds based on Anderson anions were constructed by rare-earth metal cations and not by transition metal cations [9–12]. Most compounds based on Anderson-type anions reported previously are constructed by all inorganic components without any organic unit and were usually synthesized through conventional solution methods (table 1).

Based on these considerations, in this work, choosing copper, phen, and Anderson anion as synthons through hydrothermal methods, we obtained a new Anderson-type

*Corresponding author. Email: mahy017@163.com

Journal of Coordination Chemistry
ISSN 0095-8972 print/ISSN 1029-0389 online © 2011 Taylor & Francis
DOI: 10.1080/00958972.2011.598230

Table 1. A summary of the synthetic conditions and structures of the Anderson POM-based compounds (detailed coordinate modes of a–c are shown in figure 2).

Synthesis method	Basic unit	Supported metal	Coordinate mode	Ref.
Aqueous solution	AlMo6	–	–	[13]
Aqueous solution	AlMo6	Na, Cu	a	[14]
Aqueous solution	AlMo6	Al	–	[15]
Aqueous solution	AlMo6	Cu	a	[16]
Aqueous solution	AlMo6	La	a	[7]
Aqueous solution	AlMo6	Eu	a	[17]
Aqueous solution	AlMo6/CrMo6	Cu	a	[18–21]
Aqueous solution	AlMo6/CrMo6	Na, Cu	a	[22]
Aqueous solution	CrMo6	Mn	a	[23]
Aqueous solution	CrMo6	Na, Cu	a	[24, 25]
Aqueous solution	CrMo6	Na, Zn	a	[26]
Aqueous solution	CrMo6	Na/Dy	b	[12a]
Aqueous solution	CrMo6	La	a	[27]
Aqueous solution	CrMo6	La/Ce	a	[28]
Aqueous solution	CrMo6	La, Ce, Pr, Nd	a	[29]
Aqueous solution	CrMo6	La/Nd	a	[30]
Aqueous solution	CrMo6	Ce	b	[31]
Aqueous solution	CrMo6	Ce, Sm, Eu	a	[32]
Aqueous solution	CrMo6/IMo6	Ag/Ce Ln	c	[9]
Aqueous solution	CrMo6/IMo6, IMo6	Ag	b	[33]
Aqueous solution	MnMo6/FeMo6	–	–	[34]
Aqueous solution	MnMo6	–	–	[35]
Aqueous solution	NiMo6	Ni, Ag	A	[36]
Aqueous solution	IMo6	Pr	A	[37]
Aqueous solution	IMo6	Nd	A	[38]
Aqueous solution	TeMo6	Eu, Gd, Tb, Dy, Ho, Er	A	[8]
Aqueous solution	TeMo6	Ho, Yb	B	[39]
Aqueous solution	TeMo6	La, Ce, Pr, Nd	A	[40]
Hydrothermal	TeMo6	Mn, Co, Ni, Cu, Zn La, Ce, Nd	A	[10]
Hydrothermal	TeMo6/TeMo6	Sm/Eu	A	[11]

POM organic–inorganic hybrid compound $[Cu(phen)H_2O]_2[CrH_5Mo_6O_{24}] \cdot 5H_2O$ (**1**). Its electrochemical and electroactivity properties were studied.

2. Experimental

2.1. *Materials and general procedures*

All chemicals were used as purchased without purification. IR spectrum was recorded from 4000 to 400 cm^{-1} on an Alpha Centaurt FT/IR spectrophotometer using KBr pellets. Thermal stability analysis was performed on a Perkin Elmer Diamond TG-DTA 6300 thermal analyzer in N_2 atmosphere with a heating rate of 10°C min^{-1}. Electrochemical experiments were performed with a CHI 660 Electrochemical Workstation in a conventional three-electrode electrochemical cell using **1** modified carbon paste electrode (**1**-CPE) as the working electrode, twisted platinum wire as the auxiliary electrode, and Ag/AgCl reference electrode in aqueous media. Fluorescence spectra were performed with a Perkin Elmer LS55 luminescence spectrometer using a 150 W xenon lamp as excitation source.

2.2. *Synthesis of [Cu(phen)H$_2$O]$_2$[CrH$_5$Mo$_6$O$_{24}$]·5H$_2$O (1)*

A mixture of $Na_2MoO_4 \cdot 2H_2O$ (0.45 g, 1.86 mmol), $CrCl_3 \cdot 6H_2O$ (0.2 g, 0.75 mmol), phen (0.04 g, 0.2 mmol), $CuCl_2 \cdot 2H_2O$ (0.05 g, 0.2 mmol), and H_2O (10 mL) was stirred for 30 min in air until it was homogeneous and the pH was adjusted by HCl (3 mol L^{-1}) to 1.8. The mixture was sealed in a 23 mL Teflon-lined stainless-steel container, which was heated to 165°C under autogenous pressure for 4 days. After slow cooling to room temperature at a rate of 10°C h^{-1}, bluish crystals were collected, washed with distilled water, and dried at room temperature (36% yield based on Mo). Elemental analysis: $C_{24}N_4O_{31}H_{35}CrCu_2Mo_6$ (**1**) (1630.28). Anal. Calcd for **1** (%): C, 17.68; H, 2.16; N, 3.44. Found (%): C, 16.92; H, 2.12; N, 3.39.

2.3. *Preparation of 1 modified CPE (1-CPE)*

The **1**-CPE was prepared by mixing 0.02 g of **1** with 0.3 g graphite power in an agate mortar and furbishing to achieve a uniform mixture. Then to the mixture 0.05 mL paraffin oil was added and stirred with a glass rod to get a sticky mixture. The resulting paste was packed in a glass tube (3 mm diameter) and a copper rod was inserted through one end of the tube, and pressed down tightly against a sheet of weighing paper. The other end was polished on the weighing paper to create a smooth surface.

2.4. *X-ray crystallography*

The crystal data for **1** were collected on a Bruker SMART-CCD diffractometer with Mo-Kα monochromatic radiation ($\lambda = 0.71073$ Å) at 293 K. The structure was solved by direct methods and refined by full-matrix least-squares on F^2 using the SHELXTL crystallographic software [41, 42]. Organic hydrogens were generated geometrically. Hydrogens of water in **1** could not be introduced in the refinement but were included in the structure factor calculation. The crystal data and structure refinement of **1** are summarized in table 2.

Table 2. Crystal data and structure refinement for **1**.

Empirical formula	$C_{24}N_4O_{31}H_{35}CrCu_2Mo_6$
Formula weight	1630.28
Temperature (K)	293(2)
Crystal system	Triclinic
Space group	$P\bar{1}$
Unit cell dimensions (Å, °)	
a	8.3856(5)
b	9.2366(5)
c	14.7623(8)
α	87.6400(10)
β	74.4400(10)
γ	72.4270(10)
Volume (Å^3), Z	1049.11(10), 1
Calculated density (Mg m^{-3})	2.668
Absorption coefficient (mm^{-1})	3.091
F(000)	820
Crystal size (mm^3)	0.200 × 0.160 × 0.100
θ range for data collection (°)	2.65–28.29
Reflections collected/unique	8788/4787 [R(int) = 0.0155]
Final R indices [$I > 2\sigma(I)$]	$R_1 = 0.0293$, $wR_2 = 0.0792$

3. Results and discussion

3.1. *Crystal structures*

Single-crystal X-ray diffraction analysis reveals that **1** consists of $[CrH_5Mo_6O_{24}]^{4-}$ (abbreviated as $CrMo_6$), copper cations, and 1,10-phenanthrolines (figure 1).

The building block $CrMo_6$ belongs to b-type Anderson structure, which consists of seven edge-sharing octahedra, six of which are $\{MoO_6\}$ octahedra, arranged hexagonally around the central $\{CrO\}$ octahedron. There are four distinct kinds of oxygens in the cluster, with molybdenum–oxygen distances 1.689–2.313 Å. The central Cr–O distances vary from 1.891 to 1.906 Å. The bond angles of $O–Cr–O_{cis}$ range from 84.79° to 95.21°, and bond angle of $O–Cr–O_{trans}$ is 180°. Selected bond lengths and angles of **1** are listed in table 3.

Each copper is five-coordinate with two oxygens from $[Cr(OH)_6Mo_6O_{18}]^{3-}$, two nitrogens from phen, and one H_2O. Each $CrMo_6$ anion acts as a four-coordinate inorganic ligand linking two copper centers (figure 1). We have summarized the coordination modes of Anderson polyoxoanion in reported compounds (figure 2 and table 1); the coordinate mode of Anderson polyoxoanion in **1** belongs to b-type, less observed than a-type.

A fascinating structural feature for **1** is that a 1-D chain is formed *via* $\pi\cdots\pi$ interactions with the distance of 3.674 Å between adjacent benzene rings, as shown in figure 3. Neighboring chains are linked through weak hydrogen-bonds ($O_7\cdots O_{1w} = 2.71$ Å) to achieve a 2-D supramolecular network (figure 4).

3.2. *IR spectrum*

The IR spectrum of **1** is shown in figure S1. Peaks at 950, 884, 716, 645, and 565 cm^{-1} can be regarded as characteristic of the Anderson anion $CrMo_6$. Peaks from 1700 to 1100 cm^{-1} are ascribed to phen.

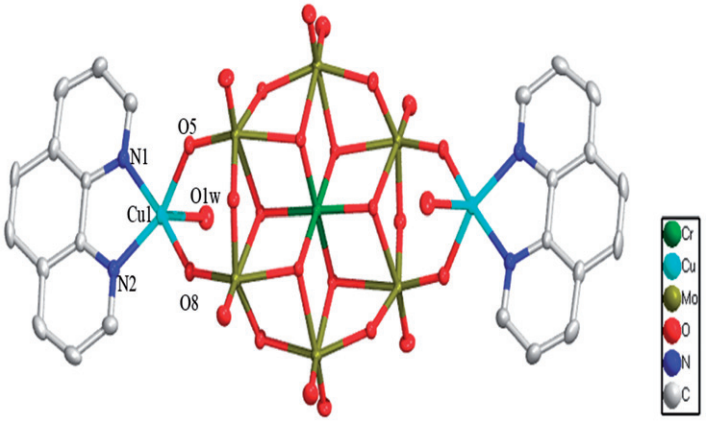

Figure 1. View of crystal structure of **1**. Hydrogens and crystal water molecules are omitted for clarity.

Table 3. Selected bond lengths (Å) and angles (°).

Atoms	Distance (Å)	Atoms	Angle (°)	Atoms	Distance (Å)	Atoms	Angle (°)
Cr(1)–O(10)	1.981(3)	O(12)#1–Cr(1)–O(12)	180.00(12)	Mo(2)–O(2)	1.703(4)	O(5)–Cu(1)–N(2)	151.50(16)
Cr(1)–O(11)	1.984(3)	O(12)#1–Cr(1)–O(10)	95.05(13)	Mo(2)–O(7)	1.708(4)	O(8)#1–Cu(1)–O(1W)	94.06(15)
Cr(1)–O(12)	1.951(3)	O(12)–Cr(1)–O(10)	84.95(13)	Mo(2)–O(9)	1.943(3)	N(1)–Cu(1)–O(1W)	96.36(17)
Cu(1)–O(8)#1	1.933(4)	O(10)–Cr(1)–O(10)#1	180.0	Mo(2)–O(6)	1.966(3)	O(5)–Cu(1)–O(1W)	90.24(14)
Cu(1)–O(1 W)	2.217(4)	O(12)#1–Cr(1)–O(11)	82.98(14)	Mo(2)–O(11)	2.225(3)	N(2)–Cu(1)–O(1 W)	117.40(16)
Cu(1)–O(5)	2.008(3)	O(12)–Cr(1)–O(11)	97.02(14)	Mo(2)–O(10)	2.313(3)	O(1)–Mo(1)–O(5)	105.06(18)
Cu(1)–N(1)	1.997(4)	O(10)–Cr(1)–O(11)	83.77(14)	Mo(3)–O(4)	1.690(4)	O(1)–Mo(1)–O(3)	100.83(17)
Cu(1)–N(2)	2.009(4)	O(10)#1–Cr(1)–O(11)	96.23(14)	Mo(3)–O(8)	1.765(3)	O(5)–Mo(1)–O(3)	98.50(16)
Mo(1)–O(1)	1.693(3)	O(11)–Cr(1)–O(11)#1	180.00(18)	Mo(3)–O(6)	1.890(4)	O(1)–Mo(1)–O(9)	100.17(16)
Mo(1)–O(3)	1.888(3)	O(8)#1–Cu(1)–N(1)	169.45(17)	Mo(3)–O(3)#1	1.994(3)	O(5)–Mo(1)–O(9)	97.19(15)
Mo(1)–O(5)	1.758(3)	O(8)#1–Cu(1)–O(5)	93.24(15)	Mo(3)–O(11)	2.139(3)	O(3)–Mo(1)–O(9)	149.43(14)
Mo(1)–O(9)	1.939(3)	N(1)–Cu(1)–O(5)	88.46(16)	Mo(3)–O(12)#1	2.298(3)	O(1)–Mo(1)–O(10)	96.16(16)
Mo(1)–O(10)	2.211(3)	O(8)#1–Cu(1)–N(2)	91.67(16)	N(1)–C(3)	1.333(7)	O(5)–Mo(1)–O(10)	157.96(14)
Mo(1)–O(12)	2.309(3)	N(1)–Cu(1)–N(2)	82.01(17)	N(1)–C(4)	1.350(6)	O(3)–Mo(1)–O(10)	83.03(14)

#1: $-x, -y+1, -z+1$.

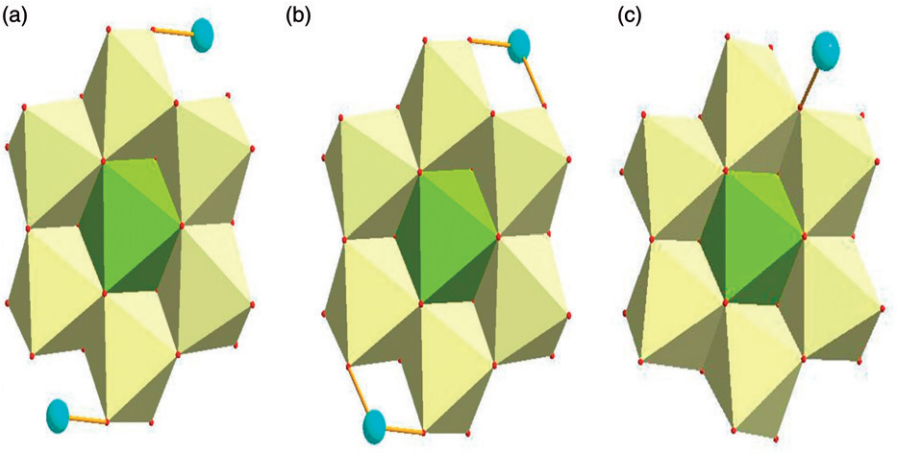

Figure 2. The observed coordination modes (a–c) of the Anderson-type anions in typical reported compounds (blue ball: metal ions).

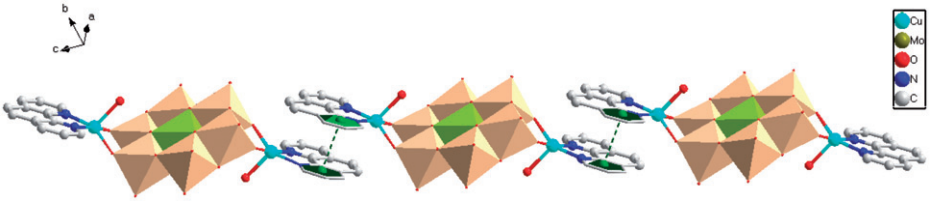

Figure 3. Polyhedral and ball-stick representation of the 1-D chain *via* $\pi\cdots\pi$ interactions in **1**.

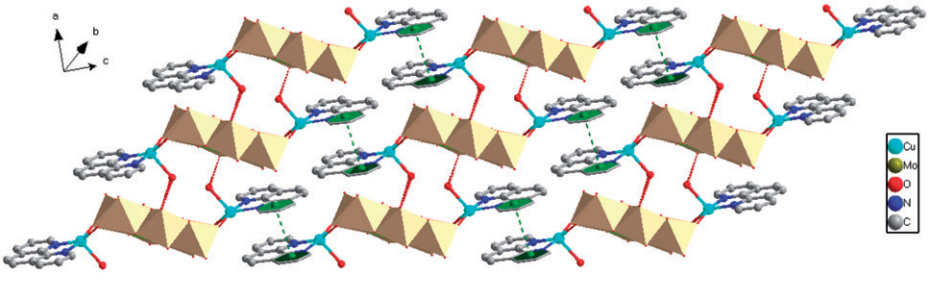

Figure 4. Polyhedral and ball-stick representation of the 2-D supramolecular network in **1**.

3.3. *Thermal analysis*

The thermal gravimetric (TG) analysis was performed under N_2 at 20°C–700°C for **1** (shown in figure S2). The TG curve of **1** exhibits two continuous weight loss steps. The first of 6.9% (Calcd 7.7%) corresponds to loss of lattice water and coordinated water. The second weight loss of 24.3% (Calcd 24.9%) is attributed to decomposition of 1,10-phenanthroline ligands and $CrMo_6$ anions. The total weight loss is 31.2%, consistent with the calculated value of 32.6% and also supporting the chemical composition of **1**.

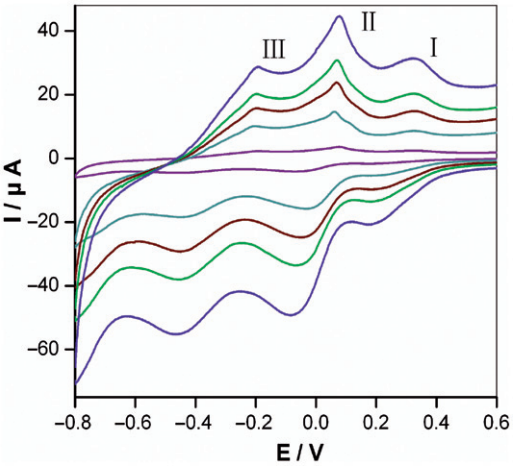

Figure 5. CVs for **1**-CPE in pH = 1.0 Na_2SO_4–H_2SO_4 buffer solution at different scan rates (inset, from inner to outer: 20, 40, 60, 80, and 100 mV s^{-1}).

3.4. *Electrochemistry*

The electrochemical behavior of **1**-modified carbon paste electrode (**1**-CPE) was investigated in H_2SO_4–Na_2SO_4 buffer solution (pH = 1.0) at different scan rates. As shown in figure 5, there are three pairs of reversible redox peaks (I–I′, II–II′, III–III′) from +0.6 to −0.8 V, with the mean peak potentials $E_{1/2} = (E_{pc} + E_{pa})$ at 0.26, 0.01, and −0.33 V (scan rate: 100 mV s^{-1}). The first pair is the redox process of Cu in the compound, and the last two pairs are ascribed to redox of Mo in the $CrMo_6$ polyanions [43–45]. As shown in the inset of figure 5, the anodic peak current increases with increasing scan rate, which is consistent with surface-confined reaction.

3.5. *Electrocatalytic activity*

POMs have been exploited extensively in electrocatalytic reactions and further applications as biosensors and fuel cells [46, 47]. Here, the reductions of hydrogen peroxide and iodate were chosen as test reactions to study the electrocatalytic activity of **1**. As shown in figure 6, **1**-CPE displays good electrocatalytic activity toward reduction of hydrogen peroxide in pH = 1.0 H_2SO_4–Na_2SO_4 buffer solution. With addition of hydrogen peroxide, the II and III cathodic peak currents, especially the third one, increased, while the corresponding anodic peak currents decreased markedly. The nearly equal current steps for each addition of hydrogen peroxide demonstrate stable and efficient electrocatalytic activity of **1** immobilized in the CPE. The **1**-CPE also exhibited remarkable electrocatalytic reduction on iodate in the buffer solution as shown in figure 7. Clearly, with gradual addition of IO_3^- to the buffer solution, all cathodic peak currents, especially the first one, increased and the corresponding anodic currents decreased dramatically, showing that **1** has very high and larruping electrocatalytic activity.

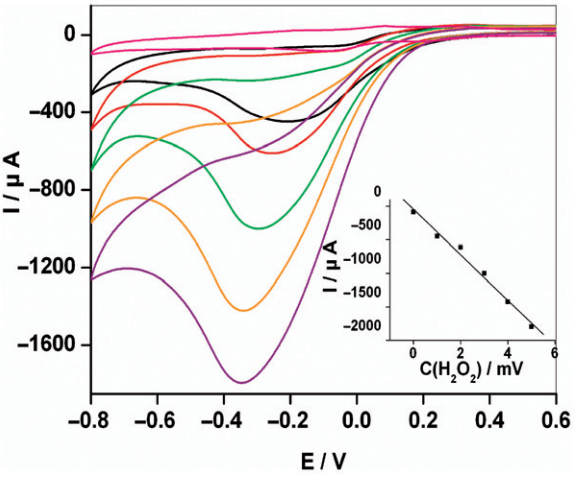

Figure 6. CVs of electrocatalytic reduction of H_2O_2 by **1**-CPE in pH = 1.0 H_2SO_4–Na_2SO_4 buffer solution with H_2O_2: in various concentrations: 1, 2, 3, 4, 5 mmol L^{-1}, scan rate: 100 mV s^{-1}. The inset shows the variation of the catalytic currents of II (I_c) with H_2O_2 concentration.

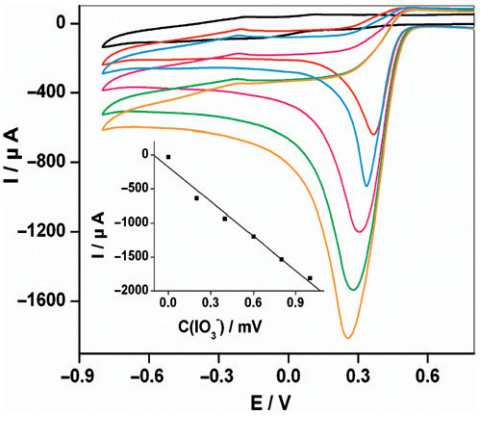

Figure 7. CVs of electrocatalytic reduction of IO_3^- by **1**-CPE in pH = 1.0 H_2SO_4–Na_2SO_4 buffer solution with IO_3^-: in various concentrations: 0.2, 0.4, 0.6, 0.8, 1.0 mmol L^{-1}, scan rate: 100 mV s^{-1}. The inset shows the variation of the catalytic currents of III (I_c) with IO_3^- concentration.

Normally electrocatalysis activity of POM toward oxidation or reduction of substrates can be evaluated by calculating the catalytic efficiency using the equation [48]:

$$\mathrm{CAT} = 100\% \times [I\mathrm{p(POM,\ substrate)} - I\mathrm{p(POM)}]/I\mathrm{p(POM)}, \quad (1)$$

where Ip(POM) and Ip(POM, substrate) are the catalytic currents of the POM in the absence and presence of substrate, respectively. To make a comparison between **1**-CPE in our work and some related molybdenum-based POM hybrids in previously

Table 4. Catalytic efficiencies of the modified electrode used in this study and comparison to related modified electrodes.

Substrate	CAT of **1**-CPE (conc. substrate)	CAT of PANI $SiMo_{12}$ (conc. substrate)	CAT of PANI P_2Mo_{18} (conc. substrate)	CAT of $(Hcpy)_6H_2[PMo_{12}O_{40}]$ (conc. substrate)
H_2O_2	377% (1 mmol L^{-1})	–	–	29% (15 mmol L^{-1}) [49]
IO_3^-	915% (0.2 mmol L^{-1})	433% (0.3 mmol L^{-1}) [50]	455% (2 mmol L^{-1}) [51]	–

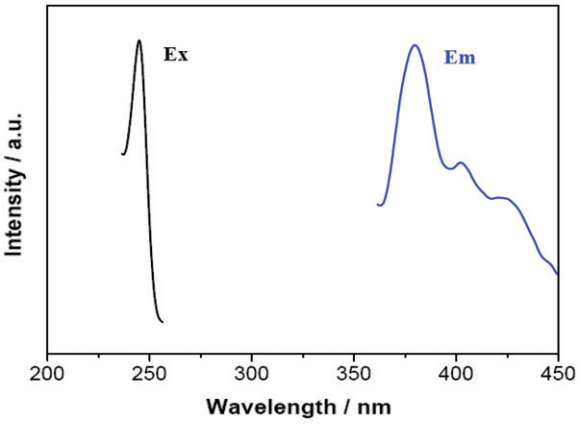

Figure 8. Luminescent spectrum of **1** in the solid state at room temperature. Ex = excitation, Em = emission.

reported papers, the catalytic efficiencies of Mo-based modified electrodes for the reduction of hydrogen peroxide and iodate were calculated and are listed in table 4. The *I*p values were obtained from peak II of figure 6 and peak III of figure 7 at a scan rate of 100 mV s^{-1}. As seen in table 4, the catalytic efficiency for **1**-CPE is much higher than the related Mo-based modified electrodes for the reduction of hydrogen peroxide and iodate. These results suggest that **1** has potential applications in the detection of hydrogen peroxide and iodate.

3.6. *Luminescence properties*

Inorganic–organic hybrid coordination polymers, especially comprising d^{10} metal centers and aromatic-containing systems, have been investigated for attractive fluorescence properties and potential applications as new luminescent materials. In this work, photoluminescence of **1** was investigated in the solid state at room temperature. Upon excitation at 245 nm, **1** shows strong emission at 380 nm (figure 8). The emission peak of free phen is at 383 nm [23]. In comparison with phen, the origin of the emission for **1** can be tentatively attributable to a joint contribution of ligand-to-metal charge transfer (LMCT).

4. Conclusion

A new compound with 2-D supramolecular network has been isolated, presenting an unusual example of Anderson polyoxoanion-based compound synthesized under hydrothermal conditions. Considering that the hydrothermal synthesis is a powerful method for obtaining new compounds, we will focus on expanding this method to construct new Anderson polyoxoanion-based compounds.

Supplementary material

Crystallographic data for **1** have been deposited in the Cambridge Crystallographic Data Center with CCDC Number 783480.

Acknowledgments

This work was financially supported by the National Science Foundation of China (No. 21071038), Science and Technology Innovation Foundation of Harbin (No. 2010RFLXG004), Heilongjiang Postdoctoral Science Foundation (No. LBH-Q09069), and Excellent Academic Leader Program of Harbin University of Science and Technology.

References

[1] C.Y. Sun, S.X. Liu, D.D. Liang, K.Z. Shao, Y.H. Ren, Z.M. Su. *J. Am. Chem. Soc.*, **131**, 1883 (2009).
[2] A. Müller, F. Peters. *Chem. Rev.*, **98**, 239 (1998).
[3] J.T. Rhule, C.L. Hill, D.A. Judd. *Chem. Rev.*, **98**, 327 (1998).
[4] (a) M.I. Khan, E. Yohannes, R.J. Doedens. *Inorg. Chem.*, **42**, 3125 (2003); (b) Y.Z. Fu. *J. Coord. Chem.*, **63**, 1856 (2010).
[5] (a) A.X. Tian, J. Ying, J. Peng, J.Q. Sha, H.J. Pang, P.P. Zhang, Y. Chen, M. Zhu, Z.M. Su. *Cryst. Growth Des.*, **8**, 3717 (2008); (b) J.P. Wang, Y.Q. Feng, J.W. Zhao, P.T. Ma, X.F. Zhang, J.Y. Niu. *J. Coord. Chem.*, **62**, 3754 (2009); (c) J.Q. Sha, J. Peng, Y.Q. Lan, Z.M. Su, H.J. Pang, A.X. Tian, P.P. Zhang, M. Zhu. *Inorg. Chem.*, **47**, 5145 (2008).
[6] (a) G.L. Guo, Y.Q. Xu, B.K. Chen, C.W. Hu. *J. Coord. Chem.*, **64**, 1032 (2011); (b) T. Yamase, H. Naruke. *J. Phys. Chem. B*, **103**, 8850 (1999).
[7] V. Shivaiah, P.V.N. Reddy, L. Cronin, S.K. Das. *J. Chem. Soc., Dalton Trans.*, 3781 (2002).
[8] D. Drewes, E.M. Limanski, B. Krebs. *J. Chem. Soc., Dalton Trans.*, 2087 (2004).
[9] H.Y. An, Y.G. Li, D.R. Xiao, E.B. Wang, C.Y. Sun. *Cryst. Growth Des.*, **6**, 1107 (2006).
[10] B. Gao, S.X. Liu, L.H. Xie, M. Yu, C.D. Zhang, C.Y. Sun, H.Y. Cheng. *J. Solid State Chem.*, **179**, 1681 (2006).
[11] Y. Liu, S.X. Liu, R.G. Cao, H.M. Ji, S.W. Zhang, Y.H. Ren. *J. Solid State Chem.*, **181**, 2237 (2008).
[12] (a) H.Y. An, D.R. Xiao, E.B. Wang, C.Y. Sun, Y.G. Li, L. Xu. *J. Mol. Struct.*, **751**, 184 (2005); (b) H.Y. Wang, C.J. Zhang, C.H. Zhang, Q. Tang, Y.G. Chen. *J. Coord. Chem.*, **64**, 1481 (2011).
[13] G.M. Sheldrick. *SHELXL-97, Program for Crystal Structure Refinement*, University of Göttingen, Germany (1997).
[14] G.M. Sheldrick. *SHELXS-97, Program for Solution of Crystal Structures*, University of Göttingen, Germany (1997).
[15] X.D. Yang, Y.G. Chen, M. Mirzaei, A.R. Salimi, F. Yao. *Inorg. Chem. Commun.*, **12**, 195 (2009).

[16] S.Z. Li, P.T. Ma, J.P. Wang, Y.Y. Guo, H.Z. Niu, J.W. Zhao, J.Y. Niu. *CrystEngComm*., **12**, 1718 (2010).
[17] Y.S. Zhou, J.B. Yin, L.J. Zhang. *J. Mol. Struct*., **920**, 61 (2009).
[18] V. Shivaiah, M. Nagaraju, S.K. Das. *Inorg. Chem*., **42**, 6604 (2003).
[19] R.G. Cao, S.X. Liu, L.H. Xie, Y.B. Pan, J.F. Cao, Y. Liu. *Inorg. Chim. Acta*, **361**, 2013 (2008).
[20] R.G. Cao, S.X. Liu, L.H. Xie, Y.B. Pan, J.F. Cao, Y.H. Ren, L. Xu. *Inorg. Chem*., **46**, 3541 (2007).
[21] R.G. Cao, S.X. Liu, Y. Liu, Q. Tang, L. Wang, L.H. Xie, Z.M. Su. *J. Solid State Chem*., **182**, 49 (2009).
[22] V. Shivaiah, S.K. Das. *Inorg. Chem*., **44**, 8846 (2005).
[23] S.W. Zhang, Y.X. Li, Y. Liu, R.G. Cao, C.Y. Sun, H.M. Ji, S.X. Liu. *J. Mol. Struct*., **920**, 284 (2009).
[24] P.P. Zhang, J. Peng, A.X. Tian, J.Q. Sha, H.J. Pang, Y. Chen, M. Zhu, Y.H. Wang. *J. Mol. Struct*., **931**, 50 (2009).
[25] Q. Wu, W.L. Chen, D. Liu, C. Liang, Y.G. Li, S.W. Lin, E.B. Wang. *Dalton Trans*., 56 (2011).
[26] H.Y. An, Y.Q. Guo, Y.G. Li, E.B. Wang, J. Lv, L. Xu, C.W. Hu. *Inorg. Chem. Commun*., **7**, 521 (2004).
[27] H.Y. An, T.Q. Xu, E.B. Wang, C.G. Meng. *Inorg. Chem. Commun*., **10**, 1453 (2007).
[28] H.Y. An, Z.B. Han, T.Q. Xu, C.G. Meng, E.B. Wang. *Inorg. Chem. Commun*., **11**, 914 (2008).
[29] H.Y. An, Y. Lan, Y.G. Li, E.B. Wang, N. Hao, D.R. Xiao, L.Y. Duan, L. Xu. *Inorg. Chem. Commun*., **7**, 356 (2004).
[30] H.Y. An, D.R. Xiao, E.B. Wang, Y.G. Li, X.L. Wang, L. Xu. *Eur. J. Inorg. Chem*., 854 (2005).
[31] H.Y. An, D.R. Xiao, E.B. Wang, Y.G. Li, L. Xu. *New J. Chem*., **29**, 667 (2005).
[32] H.Y. An, D.R. Xiao, E.B. Wang, C.Y. Sun, L. Xu. *J. Mol. Struct*., **743**, 117 (2005).
[33] J. Li, X.H. Yu, H.F. Wang, K. Xu, X.Y. Wu, L. Hou, J. Li. *Transition Met. Chem*., **31**, 770 (2006).
[34] D.M. Shi, F.X. Ma, C.J. Zhang, S. Lu, Y.G. Chen. *Z. Anorg. Allg. Chem*., **634**, 758 (2008).
[35] H.Y. An, Y.G. Li, E.B. Wang, D.R. Xiao, C.Y. Sun, L. Xu. *Inorg. Chem*., **44**, 6062 (2005).
[36] J. Zhang, J. Hao, Y.G. Wei, F.P. Xiao, P.C. Yin, L.S. Wang. *J. Am. Chem. Soc*., **132**, 14 (2010).
[37] Y.F. Song, D.L. Long, L. Cronin. *CrystEngComm*., **12**, 109 (2010).
[38] F.X. Liu, C.M. Roch, D. Dambournet, A. Acker, J. Marrot, F. Sécheresse. *Eur. J. Inorg. Chem*., 2191 (2008).
[39] H.Y. An, E.B. Wang, D.R. Xiao, Y.G. Li, L. Xu. *Inorg. Chem. Commun*., **8**, 267 (2005).
[40] H.Y. An, Y.G. Li, E.B. Wang. *J. Coord. Chem*., **59**, 379 (2006).
[41] D. Drewes, B. Krebs. *Z. Anorg. Allg. Chem*., **631**, 2591 (2005).
[42] D. Drewes, E.M. Limanski, B. Krebs. *Eur. J. Inorg. Chem*., 4849 (2004).
[43] A.X. Tian, J. Ying, J. Peng, J.Q. Sha, Z.G. Han, J.F. Ma, Z.M. Su, N.H. Hu, H.Q. Jia. *Inorg. Chem*., **47**, 3274 (2008).
[44] H.J. Pang, J. Peng, C.J. Zhang, Y.G. Li, P.P. Zhang, H.Y. Ma, Z.M. Su. *Chem. Commun*., 5097 (2010).
[45] B. Keita, E. Abdeljalil, L. Nadjo, R. Contant, R. Belgiche. *Electrochem. Commun*., **3**, 56 (2001).
[46] B. Keita, P. de Oliveira, L. Nadjo, U. Kortz. *Chem. Eur. J*., **13**, 5480 (2007).
[47] C. Pichon, P. Mialane, A. Dolbecq, J. Marrot, E. Rivière, B. Keita, L. Nadjo, F. Secheresse. *Inorg. Chem*., **46**, 5292 (2007).
[48] B. Keita, A. Belhouari, L. Nadjo, R. Contant. *J. Electroanal. Chem*., **381**, 243 (1995).
[49] Z.G. Han, Y.Z. Gao, J.Y. Wang, C.W. Hu. *Z. Anorg. Allg. Chem*., **635**, 2665 (2009).
[50] H.Y. Ma, T. Dong, G. Wang, W. Zhang, F.P. Wang, X.D. Wang. *Electroanalysis*, **18**, 2475 (2006).
[51] J.Y. Qu, X.Q. Zou, B.F. Liu, S.J. Dong. *Anal. Chim. Acta*, **599**, 51 (2007).